XLI CILAMCE
XLI Ibero-Latin American Congress on Computational Methods in Engineering
16-19 November, 2020 FOZ DO IGUAÇU PARANÁ - BRAZIL

A LOCAL MESHLESS ANALYSIS OF DYNAMICS PROBLEMS

Flávio Mendonça, Wilber Vélez, Fernando Martins, Amanda Araújo, Artur Portela

Department of Civil Engineering, Faculty of Technology, University of Brasília
Asa Norte, 70910-900, Brasília – DF, Brazil
flavioprimeiro@yahoo.com.br, wilbervelez@hotmail.com,

Abstract. This paper is concerned with new formulations of local meshfree numerical method, for the solution of dynamic problems in linear elasticity, Integrated Local Mesh Free (ILMF) method. The key attribute of local numerical methods is the use of a modeling paradigm based on a node-by-node calculation, to generate the rows of the global system of equations of the body discretization. In the local domain, assigned to each node of a discretization, the work theorem is kinematically formulated, leading thus to an equation of mechanical equilibrium of the local node, that is used by local meshfree method as the starting point of the formulation. The main feature of this paper is the use of a linearly integrated local form of the work theorem. The linear reduced integration plays a key role in the behavior of local numerical methods, since it implies a reduction of the nodal stiffness which, in turn, leads to an increase of the solution accuracy. As a consequence, the derived meshfree and finite element numerical methods become fast and accurate, which is a feature of paramount importance, as far as computational efficiency of numerical methods is concerned. The cantilever beam was analyzed with this technique, in order to assess the accuracy and efficiency of the new local numerical method for dynamic problems with regular and irregular nodal configuration. The results obtained in this work are in perfect agreement with Mesh-Free Local Petrov-Galerkin (MLPG) and the Finite Element Method (FEM) solutions.

Keywords: Local Meshfree numerical method, dynamic problems, Moving Least Squares (MLS), Integrated Local Mesh Free (ILMF), Mesh-Free Local Petrov-Galerkin (MLPG).

1 Introduction

Numerical methods based on grids, as the finite element method (FEM), are widely used in engineering and science. Grid based methods required high quality meshes when solving fracture mechanics problems, with material discontinuities, nonlinear problems, with large displacements, where excessive mesh distortion takes place. On the other hand, meshfree methods were developed with the expectation of providing more adaptive, accurate and stable numerical solutions, to deal with problems where conventional grid-based methods are not well suited, Daxini and Prajapati [1]. In general, their formulation is based in the weighted residual method, see, Finalyson [2].

Different meshless methods have been developed during the last 20 years, as reported by Chen *et. al.* [3]. Some of these methods, based on a weighted residual global weak form, were applied in solid mechanics, such as the diffuse element method (DEM), presented by Nayroles *et. al.* [4], the reproducing kernel particle method (RKPM), presented by Liu *et. al.* [5], and the element free Galerkin (EFG), Belytschko *et. al.* [6]. Other methods emerged based on weighted residual local weak forms, such as the meshless local Petrov-Galerkin method (MLPG), presented by Atluri and Zhu [7], the meshless local boundary integral equation method (MLBIE), see Zhu [8], the local point interpolation method (LPIM), presented by Liu and Gu [9], the local radial point interpolation method (LRPIM), presented by Liu *et. al.* [10], the meshless finite volume method (FVM), presented by Atluri *et. al.* [11], the rigid body displacement meshfree method (RBDMF) and the generalized strain meshfree method (GSMF), both presented by Oliveira and Portela [12].

MLPG, the most popular of these methods, is based on a moving least squares approximation (MLS). The main difference of the MLPG method to other global meshless methods, such as EFG or RKPM, is that local weak forms are used for integration on overlapping regular shaped local subdomains, instead of a global weak form. Consequently, the method does not require the use of a background global mesh, but only a background local grid, which usually has a simple shape. Using the MLS approximation, the ILMF model implements a linear reduced numerical integration, on the boundaries of the local integration domain associated to each node, with one single point per segment, which leads to a point-wise discrete form that represents equilibrium of tractions defined at integration points. The reduced integration, a key feature of this formulation, induces a reduction of the nodal stiffness which, in turn, increases the solution accuracy, as a consequence of the theorem of the minimum total potential energy.

This paper is concerned on the size effect of the irregularity of the nodal arrangement, referred to by the irregularity parameter (C_n), when the discretization is considered with fixed values of the local support domain (α_s) and the local quadrature domain (α_q). The paper presents a comparison of the relative error for frequencies natural for three different irregular nodal distributions used to solve the benchmark problem of the Timoshenko cantilever beam. Results obtained with the ILMF model are compared with the results of the MLPG, as well as the Finite Element Method (FEM) solution. Optimal results were obtained.

2 Methodology

Let Ω be the domain of a body and Γ its boundary, subdivided in Γ_u and Γ_t that is $\Gamma = \Gamma_u \cup \Gamma_t$; in the Fig. 1 show the nodal points P, Q and R have corresponding local domains Ω_P, Ω_Q, and Ω_R. The general fundamental boundary value problem of linear elastostatics aims to determine the distribution of stresses $\boldsymbol{\sigma}$, strains $\boldsymbol{\varepsilon}$ and displacements $\mathbf{u}$, throughout the body, when it has constrained displacements $\bar{\mathbf{u}}$, on Γ_u and it is loaded by an external system of distributed surface and body forces with densities denoted, respectively by $\bar{\mathbf{t}}$, on Γ_t and $\mathbf{b}$, in Ω.

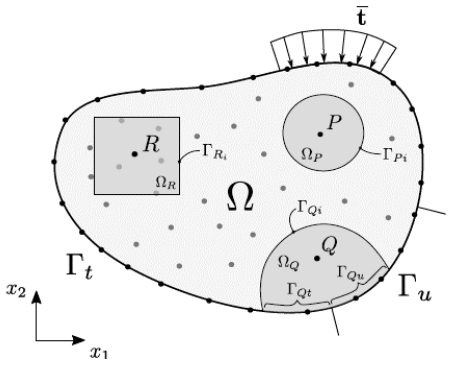

Figure 1. Global domain Ω and the local domains Ω_P, Ω_Q and Ω_R, with boundary $\Gamma = \Gamma_u \cup \Gamma_t$ represented.

The solution of these problem is a totally admissible elastic field that simultaneously satisfies the kinematic admissibility of the strains and the static admissibility of the stresses. If this solution exists, it can be shown that it is unique, provided linearity and stability of the material are admitted. Such is the Kirchhoff's theorem, on the uniqueness of solutions of the elastostatic boundary value problem, Kirchhoff [13]. For the sake of generality, the solution of the posed problem is derived through the work theorem.

In the body's domain Ω consider a statically admissible stress field $\boldsymbol{\sigma}$, which is any stress field that satisfies the equilibrium with the system of applied external forces which therefore satisfies

$$\mathbf{L}^T \sigma + b = 0, \tag{1}$$

in the domain Ω, with boundary conditions

$$\mathbf{t} = \mathbf{n}\boldsymbol{\sigma} = \bar{\mathbf{t}}, \tag{2}$$

on the static boundary Γ_t, in which **L** is a matrix differential operator; **t** is the vector of traction components; $\bar{\mathbf{t}}$ is the vector of the prescribed tractions and **n** is the matrix of the components of the unit outward normal to the boundary.

In the domain Ω consider an arbitrary local domain Ω_Q, assigned to a reference point $Q \in \Omega_Q$, with local boundary $\Gamma = \Gamma_{Qi} \cup \Gamma_{Qt} \cup \Gamma_{Qu}$, Γ_{Qi}, in which Γ_{Qi} is the interior local boundary, while Γ_{Qt} and Γ_{Qu} are local boundaries that share the global boundaries, respectively the static boundary Γ_t and the kinematic boundary Γ_u, as represented in Fig. 1. The work theorem will be used as a local form that is valid in the arbitrary local domain Ω_Q. Due to its arbitrariness, this local domain $\Omega_Q \cup \Gamma_Q \in \Omega \cup \Gamma$ can be overlapping with other similar sub-domains that can be defined in the body.

The work theorem establishes an energy relationship, valid in an arbitrary local domain $\Omega_Q \in \Omega$, between two independent elastic fields that can be defined in the body which are, respectively a statically admissible stress field that satisfies equilibrium with a system of external forces, and a kinematically admissible strain field that satisfies the compatibility with a set of constrained displacements. Derived as a weighted residual statement, the work theorem serves as a unifying basis for the formulation on numerical models Continuum Mechanics, Brebbia and Tottenham [14]. Expressed as an integral local form, defined in the local domain Ω_Q, the work theorem can be written in a compact form, simply as

$$\int_{\Gamma_Q} \mathbf{t}^T \mathbf{u}^* d\Gamma + \int_{\Omega_Q} \mathbf{b}^T \mathbf{u}^* d\Omega = \int_{\Omega_Q} \boldsymbol{\sigma}^T \varepsilon^* d\Omega, \tag{3}$$

in which the stress field $\boldsymbol{\sigma}$ and the strain field $\boldsymbol{\varepsilon}^*$ are not linked by any constitutive relationship and therefore, they are independent of each other, see Olivera and Portela [12]. The statically admissible stress field $\boldsymbol{\sigma}$ can be any stress field that is in equilibrium with the system of applied external forces, therefore satisfying eqs. (1) e (2), which is not necessarily the stress field that the system of applied external forces introduces in the body. The kinematically admissible strain field $\boldsymbol{\varepsilon}^*$ can be any strain field defined in the body, generated by continuous displacements $\mathbf{u}^*$ with small derivatives, compatible with an arbitrary set of constraints specified on the kinematic boundary, which is not necessarily the strain field that actually settles in the body. Finally, the local domain Ω_Q is any arbitrary sub-domain of the body, associated to the reference point Q, as represented in Fig. 1, where the independent fields $\boldsymbol{\sigma}$ and $\boldsymbol{\varepsilon}^*$ can be defined.

Kinematic formulations consider, in the work theorem, a particular and convenient specification of the kinematically admissible strain field, leading thus to an equation of mechanical equilibrium that is used to generate the stiffness matrix of the numerical model. Bearing in mind the essential feature of the work theorem, which is the complete independence of the stress field $\boldsymbol{\sigma}$ and the strain field $\boldsymbol{\varepsilon}^*$, the strain field can be conveniently defined by a rigid-body displacement that can be defined as

$$\mathbf{u}^*(\mathrm{x}) = \mathbf{c}, \tag{4}$$

where **C** is a constant vector that conveniently leads to null strains that is

$$\boldsymbol{\varepsilon}^*(\mathrm{x}) = \mathbf{0}. \tag{5}$$

When this kinematic formulation is considered, the local form of the work theorem, eq. (3), simply leads to the equation

$$\int_{\Gamma_Q - \Gamma_{Qt}} \mathbf{t}\, d\Gamma + \int_{\Gamma_{Qt}} \bar{\mathbf{t}}\, d\Gamma + \int_{\Omega_Q} \mathbf{b}\, d\Omega = 0, \tag{6}$$

which states an integral form of mechanical equilibrium, of tractions and body forces, in the local domain Ω_Q, are represented in Fig. 2. This equation expresses the local version of the basic Euler-Cauchy stress principle that is sometimes referred to as the defining principle of continuum mechanics.

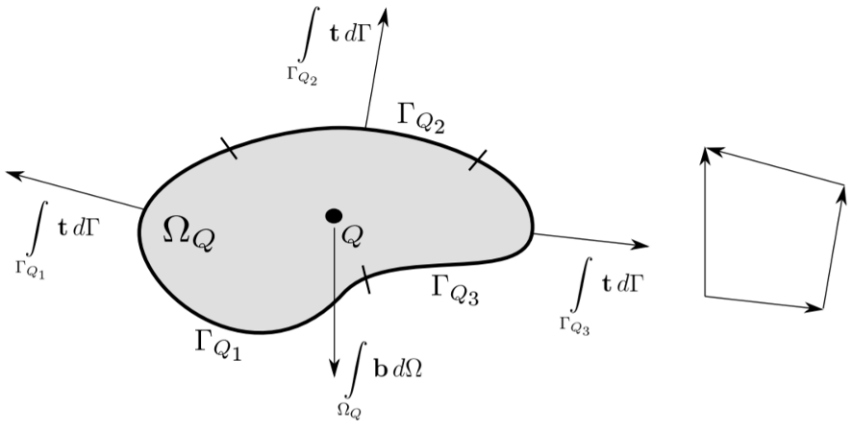

Figure 2. Schematic representation of the equilibrium of tractions and body forces, pointwisely defined at collocation points of a local form of the work theorem associated with a field node Q.

The modeling strategy, adopted to solve the actual elastic problem, considers that the stress field **σ**, required to satisfy the equilibrium with a system of external forces, is assumed as the stress field that actually settles in the body, when it is loaded by the actual system of external distributed surface and body forces, with the actual displacement constraints. Recall that the elastic field that actually settles in the body is the unique fully admissible elastic field that satisfies the given problem. Therefore, besides satisfying static admissibility, through eq. (1) and (2), that is the same as satisfying equilibrium through eq. (6), generated by the weak form eq. (3) of the work theorem, this unique fully admissible elastic field also must satisfy kinematic admissibility defined as

$$\varepsilon = \mathbf{L}\mathbf{u}, \tag{7}$$

in the domain Ω, with boundary conditions

$$\mathbf{u} = \bar{\mathbf{u}}, \tag{8}$$

on the kinematic boundary Γ_u, in which the displacement **u** is assumed continuous with small derivatives, in order to allow for geometrical linearity of the strain field ε. Hence, eq. (8), which specifies the constraints of the actual displacements, must be enforced in any numerical model, in order to provide a unique solution of the elastic problem. For the sake of simplicity, this paper considers the formulation of the ILMF model in the absence of body forces. Consequently, the nodal equations of equilibrium are always defined only on the boundary of the local domain.

The meshless method with reduce integration is based on the widely used moving least-squares (MLS) approximation, introduced by Atluri and Zhu [15]. The MLS approximation is one of the best methods to approximate data with a good accuracy. Circular or rectangular local supports centered at each nodal point can be used. In the region of a sampling point X, the domain of definition of MLS approximation is the subdomain Ω_x, where the approximation is defined, as showed in the Fig. 3.

The definition domain contains all the nodes whose MLS shape functions do not vanish at this sampling point. Therefore, the domain of influence of each node, is the union of the MLS domains of definition of all points in the local domain of the node.

Finally, local mesh free formulations use a node-by-node stiffness calculation to generate, in the domain of influence of the local node, the respective rows of the global stiffness matrix.

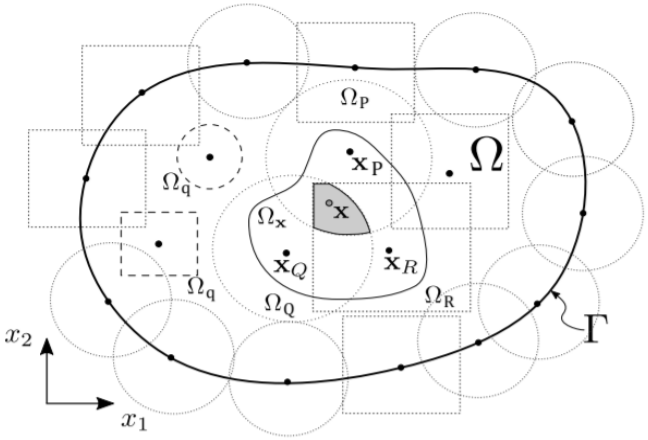

Figure 3. Representation of a global domain Ω and boundary Γ in the meshless discretization, with Xi nodes distributed within the body.

2.1 Mesh-free Local Petrov-Galerkin (MLPG)

For a nodal discretization of a body using the Mesh-free Local Petrov-Galerkin (MLPG) method, the respective system of algebraic equations is calculated, in a node-by-node process, by integrating the local form assigned to each node, eq. (6), with local domains rectangular or circular and numerical quadrature applied to each side, or quadrant, of the local domain, as schematically represented in Fig. 4.

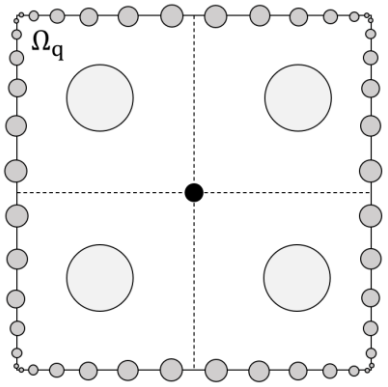

Figure 4. Schematic representation of numerical quadrature points, of local MLPG domains, for calculating the local form of the work theorem, with the formulation of rigid body displacement.

The local form of the work theorem with the rigid-body displacement, eq. (6), can be written simply as

$$-\int_{\Gamma_Q-\Gamma_{Qt}} \mathbf{t}\, d\Gamma = \int_{\Gamma_{Qt}} \bar{\mathbf{t}}\, d\Gamma + \int_{\Omega_Q} \mathbf{b}\, d\Omega \tag{7}$$

which can be written as

$$\mathbf{K}_Q \hat{\mathbf{u}} = \mathbf{F}_Q \tag{8}$$

where $\mathbf{K}_Q$, the nodal stiffness matrix associated with the Q field node, is a 2x2n matrix (n is the number of nodes included in the reference domain influence Q node which is the union of all definition MLS domains integration points in the local domain Ω_Q) given by

$$\mathbf{K}_Q = -\int_{\Gamma_Q - \Gamma_{Qt}} \mathbf{nDB}\, d\Gamma \tag{9}$$

and $\mathbf{F}_Q$ is the respective force vector given by

$$\mathbf{F}_Q = \int_{\Gamma_{Qt}} \bar{\mathbf{t}}\, d\Gamma + \int_{\Omega_Q} \mathbf{b}\, d\Omega \tag{10}$$

Consider that the problem has a total of N field nodes Q, each one associated with the respective local region Ω_Q. Assembling eq. (8), for all M interior and static – boundary field nodes leads to the global system of 2M x 2N equations

$$\mathbf{K}\hat{\mathbf{u}} = \mathbf{F}. \tag{11}$$

Finally, the remaining equations are obtained from the N – M boundary field nodes on the kinematic boundary. For a field node on the kinematic boundary, a direct interpolation method is used to impose the Kinematic boundary condition as equations

$$u_k(\mathrm{x}_j) = \sum_{i=1}^{n} \phi_i(\mathrm{x}_j)\hat{u}_{ik} = \bar{\mathbf{u}}_k, \tag{12}$$

Or, in matrix form as equations

$$\mathbf{u}_k = \sum_{i=1}^{n} \Phi_k \hat{\mathbf{u}} = \bar{\mathbf{u}}_k, \tag{13}$$

with k = 1, 2, where $\bar{\mathbf{u}}_k$ is specified nodal displacement component. Equations (12) are directly assembled into the global system of eq. (11). to build the respective nodal stiffness matrix of MLPG, it is computationally much more efficient than the other meshless methods that use domain integration, as is the case of the EFG method, presented by Belytschko et. al. (1994), or the MLPG1 and MLPG3 methods presented by Atluri and Shen (2002).

2.2 Integrated Local Mesh Free method (ILMF)

Assuming a variation linear of the tractions along each boundary segment of the local domain, the local integral form of equilibrium can be evaluated with a single quadrature point, centered on each segment of the boundary, Fig. 5. Applying this linear integration process in the Eq. (7), the following expression is obtained

$$-\frac{L_i}{n_i}\sum_{i=1}^{n_i} \bar{\mathrm{t}}_{\mathrm{x}_j} = \frac{L_t}{n_t}\sum_{j=1}^{n_t} \bar{\mathrm{t}}_{\mathrm{x}_k} + \int_{\Omega_Q} \mathbf{b}\, d\Omega \tag{14}$$

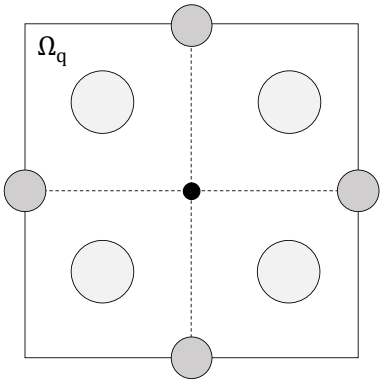

Figure 5. Schematic representation of numerical quadrature points, of local ILMF domains, for the calculation of the local form of the work theorem, with the formulation of rigid body displacement.

For a given nodal distribution, Eq. (14) can be presented as follows

$$-\frac{L_i}{n_i}\sum_{i=1}^{n_i}\mathbf{n}_{x_j}\mathbf{DB}_{x_j}\hat{\mathbf{u}}=\frac{L_t}{n_t}\sum_{j=1}^{n_t}\bar{t}_{x_k}+\int_{\Omega_Q}\mathbf{b}\ d\Omega \tag{15}$$

which can be written as

$$\mathbf{K}_Q\hat{\mathbf{u}}=\mathbf{F}_Q \tag{16}$$

where $\mathbf{K}_Q$, the nodal stiffness matrix associated with the Q field node, is a 2x2n matrix (n is the number of nodes included in the reference domain influence Q node which is the union of all definition MLS domains integration points in the local domain Ω_Q) given by

$$\mathbf{K}_Q=-\frac{L_i}{n_i}\sum_{i=1}^{n_i}\mathbf{n}_{x_j}\mathbf{DB}_{x_j}\hat{\mathbf{u}} \tag{17}$$

and $\mathbf{F}_Q$ is the respective force vector given by

$$\mathbf{F}_Q=\frac{L_t}{n_t}\sum_{j=1}^{n_t}\bar{t}_{x_k}+\int_{\Omega_Q}\mathbf{b}\ d\Omega \tag{18}$$

Consider that the problem has a total of N field nodes Q, each one associated with the respective local region Ω_Q. Assembling eq. (16), for all M interior and static – boundary field nodes leads to the global system of 2M x 2N equations

$$\mathbf{K}\hat{\mathbf{u}}=\mathbf{F}. \tag{19}$$

Finally, the remaining equations are obtained from the N – M boundary field nodes on the kinematic boundary. For a field node on the kinematic boundary, a direct interpolation method is used to impose the Kinematic boundary condition as equations

$$u_k(x_j)=\sum_{i=1}^{n}\phi_i(x_j)\hat{u}_{ik}=\bar{\mathbf{u}}_k, \tag{20}$$

Or, in matrix form as equations

$$\mathbf{u}_k=\sum_{i=1}^{n}\Phi_k\hat{\mathbf{u}}=\bar{\mathbf{u}}_k, \tag{21}$$

with k = 1, 2, where $\bar{\mathbf{u}}_k$ is specified nodal displacement component. Equations (12) are directly assembled into the global system of eq. (16).

2.3 Parameters of the Meshless Discretization

This section presents some numerical results for Cantilever beam for different nodal configurations. The effects of the size of local support and quadrature domain are analyzed and compared with exact solution.

For a generic node i, the size of the local support Ω_S and the local domain of integration Ωq are respectively given by

$$r\Omega_S=\alpha_S d_i, \tag{21}$$

$$r\Omega_q=\alpha_q d_i, \tag{22}$$

in which di represents the distance of the node i, to the nearest neighboring node; for the analysis is performed for two different values of the local support domain size (α_s = 3.5), and the local quadrature domain size (α_q = 0.5)

2.4 Irregular nodal arrangement

The nodal irregularity is generated by changing randomly the coordinates of the nodal regularity distribution by small distance, this movement can be calculated by

$$x_{1i}' = x_{1i} \pm c_n d_{x_{1i}}, \tag{23}$$

$$x_{2i}' = x_i \pm c_n d_{x_{2i}}, \tag{24}$$

in which Cn is a parameter that controls the nodal irregularity and vary randomly in the range of 0.0 and 0.3. For nodes located in the boundary there are restrictions that depend on the position of the node.

3 Dynamic Analysis

The domain Ω is represented by a set of distributed nodes, for dynamic analysis **u** is a function of space and time. Only the equations for the space coordinates are discretized. Using the MLS shape is obtaining the following discretized system equations for the *I*th field node.

$$\mathbf{M}_I \ddot{\mathbf{u}}(t) + \mathbf{C}_I \dot{\mathbf{u}}(t) + \mathbf{K}_I \mathbf{u}(t) = \mathbf{F}_I(t) \tag{25}$$

where **u** is the vector of nodal displacements (or nodal displacement parameters) for nodes in the support domain of the *I*th field node, $\mathbf{M}_I$ is the nodal mass matrix and $\mathbf{C}_I$ is the nodal damping matrix.

Equation (25) presents two linear equations for the *I*th field node, using this equation for all nodes in the entire domain Ω, and assembling all these 2N equations, it is obtained the final global system equations in the following matrix form

$$\mathbf{M}\ddot{\mathbf{U}} + \mathbf{C}\dot{\mathbf{U}} + \mathbf{K}\mathbf{U} = \mathbf{F} \tag{26}$$

Equation (26) is system equation for dynamic analyses of two-dimensional solids. Solving this equation are obtained the displacements for all field nodes and the retrieve all the stresses at any point in the problem domain.

For free vibration analysis, the aims are obtained the natural frequencies and the corresponding vibration nodes. The displacement **u** (**x**, t) can be written as a harmonic function of times as follows

$$\mathbf{u}(\mathrm{x}, \mathrm{t}) = \mathbf{\Phi}(\mathrm{x})\hat{\mathbf{u}}\sin(\omega t + \varphi) \tag{27}$$

where *w* is the natural frequency and φ is the phase of the harmonic motion and $\hat{\boldsymbol{u}}$ are the amplitude for displacement. Substituting eq. (27) in eq. (26) is obtained the final system equation in terms of the amplitudes of modal displacements for free vibration analysis.

$$(\mathbf{K} - \omega^2 \mathbf{M})\hat{\mathbf{U}} = \mathbf{0} \tag{28}$$

where $\hat{\mathbf{U}}$ is the vector amplitudes for all nodal displacements; eq. (28) can also be written in the following typical eigenvalue equation

$$(\mathbf{K} - \lambda \mathbf{M})\mathbf{q} = 0 \tag{29}$$

where $\lambda = \omega^2$ is the eigenvalue, and **q** is the eigenvector. This equation can be solved using a standard eigenvalue solver to obtain eigenvalues λ_i (i = 1, 2,…, N) and the corresponding **q.** The natural frequencies of the structures are given by $\omega_i = \sqrt{\boldsymbol{\lambda_i}}$. The vibration modes correspond to the eigenvectors.

4 Numerical Examples

The MLPG and ILMF methods were used for the free vibration analysis of the cantilever beam shown in Fig. 6. The parameters are presented in table 1. In the free vibration analyses $\alpha_s = 3.5$ was used for the local support domain and $\alpha_q = 0.5$ for local quadrature domain.

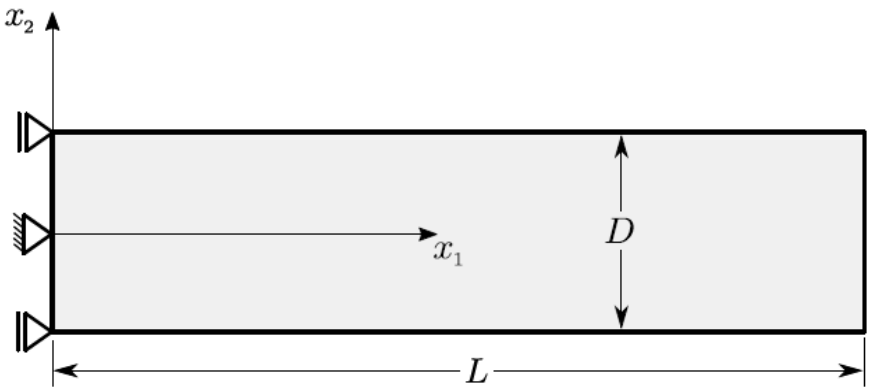

Figure 6. Cantilever beam

Table 1. Parameters of Cantilever beam

Parameters	Values
Height, D	12
Length, L	48
Thickness, t	1
Modulus of Elasticity, E	30 000000
Poisson`s Ratio, ν	0.3
Mass density	1

Three kinds of regular nodal arrangements (189, 403 and 1261) were used, Fig. 7.

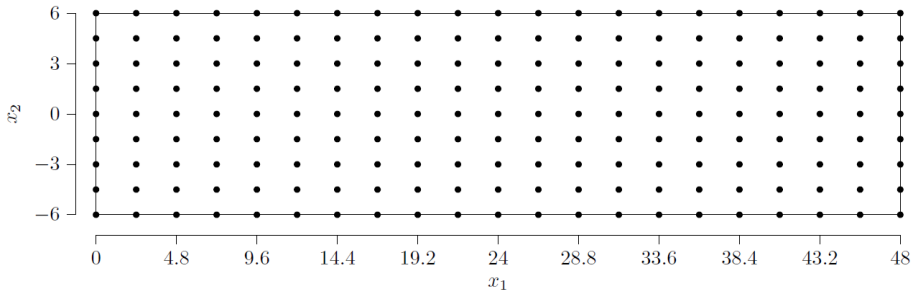

a) 21 x 9 = 189 nodes

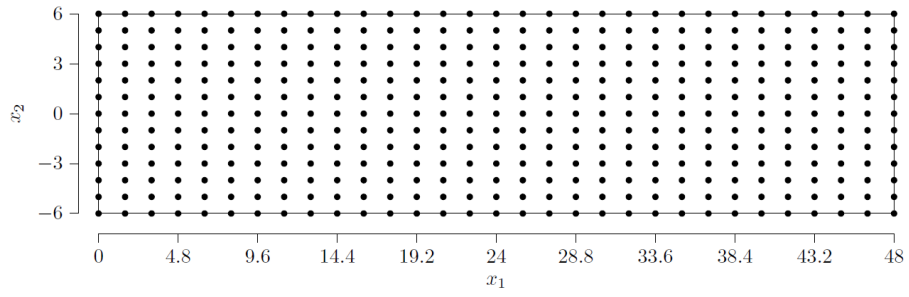

b) 31 x 13 = 403 nodes

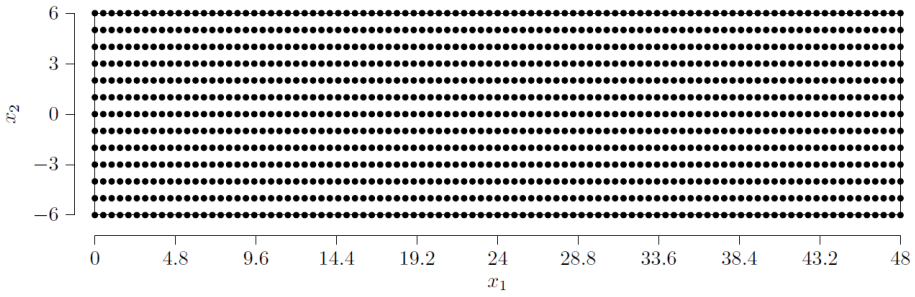

c) 97 x 13 = 1261 nodes

Figure 7. Cantilever beam

Frequencies of three nodal distributions obtained for MLPG and ILMF are listed in table 2, table 3 and table 4. The results of the FEM, Liu [16]. The relative error for the natural frequency is given, respectively by

$$r_{\varepsilon} = \frac{\|MLPG - FEM\|}{\|FEM\|} \tag{30}$$

$$r_{\varepsilon} = \frac{\|ILMF - FEM\|}{\|FEM\|} \tag{31}$$

Table 2. Natural frequencies of Cantilever Beam using MLPG and ILMF with 189 nodes

Modo	MLPG	ILMF	Reference (FEM – 4850 DOFs)	Relative error (MLPG/FEM)	Relative error (ILMF/FEM)
1	28.60	20.22	27.72	3.17E-02	2.71E-01
2	141.06	140.72	140.86	1.42E-03	9.94E-04
3	185.02	185.23	179.71	2.95E-02	3.07E-02
4	327.37	323.40	323.89	1.07E-02	1.51E-03
5	519.63	520.99	523.43	7.26E-03	4.66E-03
6	537.45	536.58	536.57	1.64E-03	1.86E-05
7	729.32	728.27	730.04	9.86E-04	2.42E-03
8	884.05	881.86	881.28	3.14E-03	6.58E-04
9	900.43	900.83	899.69	8.23E-04	1.27E-03
10	1001.18	1000.68	1000.22	9.60E-04	4.60E-04

Table 3. Natural frequencies of Cantilever Beam using MLPG and ILMF with 403 nodes

Modo	MLPG	ILMF	Reference (FEM – 4850 DOFs)	Relative error (MLPG/FEM)	Relative error (ILMF/FEM)
1	28,60	20,22	27,72	3,17E-02	2,71E-01
2	141,29	141,02	140,86	3,05E-03	1,14E-03
3	185,64	184,51	179,71	3,30E-02	2,67E-02
4	325,13	323,57	323,89	3,83E-03	9,88E-04
5	523,75	522,76	523,43	6,11E-04	1,28E-03
6	537,03	535,49	536,57	8,57E-04	2,01E-03
7	729,41	730,62	730,04	8,63E-04	7,94E-04
8	882,58	885,35	881,28	1,48E-03	4,62E-03
9	899,01	900,19	899,69	7,56E-04	5,56E-04
10	1.001,63	998,69	1.000,22	1,41E-03	1,53E-03

Table 4. Natural frequencies of Cantilever Beam using MLPG and ILMF with 1261 nodes

Modo	MLPG	ILMF	Reference (FEM – 4850 DOFs)	Relative error (MLPG/FEM)	Relative error (ILMF/FEM)
1	28,60	20,22	27,72	3,17E-02	2,71E-01
2	140,17	140,81	140,86	4,90E-03	3,55E-04
3	186,51	174,53	179,71	3,78E-02	2,88E-02
4	321,94	324,24	323,89	6,02E-03	1,08E-03
5	525,69	522,81	523,43	4,32E-03	1,18E-03
6	536,42	536,86	536,57	2,80E-04	5,40E-04
7	729,92	730,66	730,04	1,64E-04	8,49E-04
8	881,48	881,00	881,28	2,27E-04	3,18E-04
9	901,67	899,13	899,69	2,20E-03	6,22E-04
10	1.001,50	999,84	1.000,22	1,28E-03	3,80E-04

In order to visually facilitate the presentation of the data, these values are plotted in the Fig. 8.

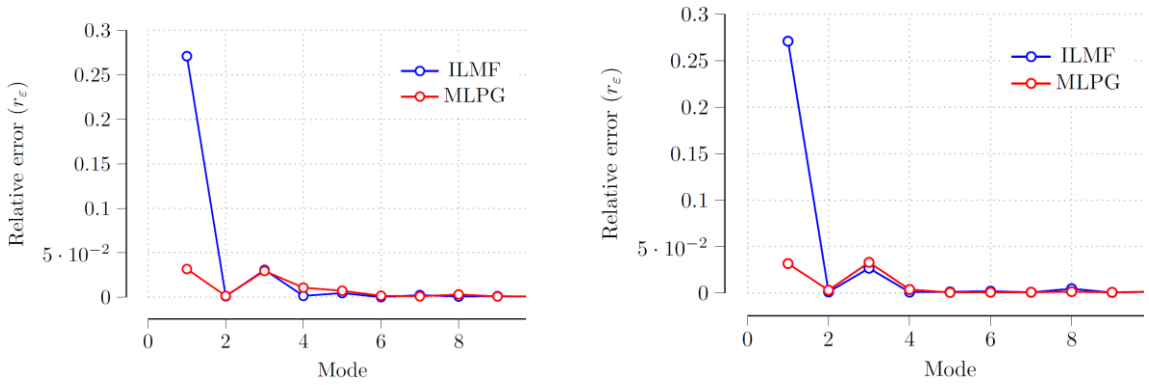

a) 189 nodes

b) 403 nodes

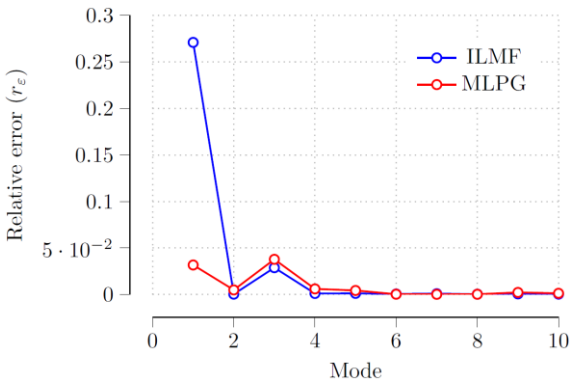

c) 1261 nodes

Figure 8. Relative error of natural frequencies for three different regular nodal arrangement.

Figure 8 shows that the first mode presented the major relative error for ILMF method regardless of the regular nodal arrangement. MLPG present a better behavior when compared with the FEM (ANSYS) results. In general, the relative error decreases when the number of nodes increases.

Table 4 presents the relative error of the natural frequencies using the MLPG method with different values for the irregularity parameter $\mathbf{C_n}$ (0.1, 0.2 and 0.3). 1261 nodes are used for these analyses.

Table 4. Relative error of Natural frequencies of Cantilever Beam using MLPG with 1261 nodes and different irregular nodal distributions

Modo	Reference (FEM – 4850 DOFs)	Relative error $C_n = 0.1$	Relative error $C_n = 0.2$	Relative error $C_n = 0.3$
1	27,72	3.19E-02	3.17E-02	3.12E-02
2	140,86	4.73E-03	4.19E-03	7.30E-03
3	179,71	3.86E-02	3.89E-02	1.51E-02
4	323,89	2.89E-03	8.53E-03	7.18E-03
5	523,43	2.61E-03	8.16E-03	1.88E-03
6	536,57	2.46E-03	2.50E-03	1.58E-03
7	730,04	4.48E-03	2.91E-04	2.51E-03
8	881,28	3.15E-04	1.34E-03	1.19E-03
9	899,69	5.36E-04	1.09E-03	4.77E-03
10	1.000,22	1.93E-03	1.54E-03	2.17E-03

Figure 9 shows the relative error of the natural frequencies of the cantilever beam using regular and irregular nodal arrangement and Fig. 10 presented the irregular nodal arrangement with the irregularity parameter C_n =0 .3, both with 1261 nodes.

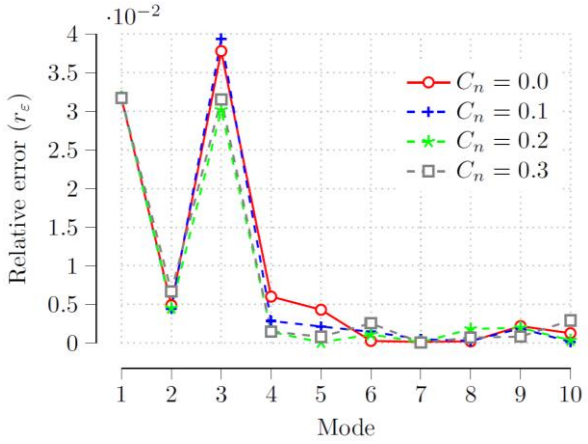

Figure 9. MLPG relative error of natural frequencies for three different value of the irregularity parameter C_n (0.1, 0.2 and 0.3) with 1261 nodes.

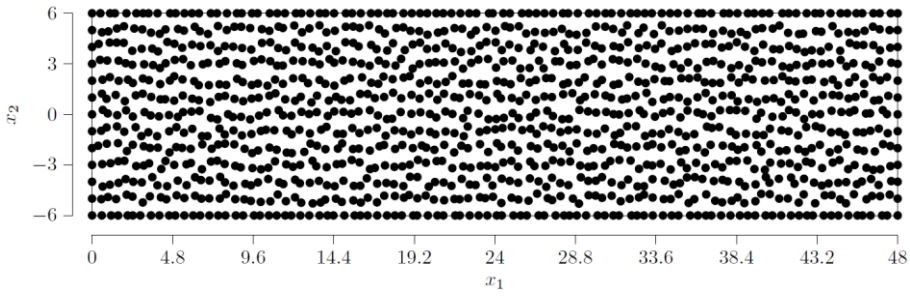

Figure 10. Irregular nodal arrangement with Cn = 0.3 and 1261 nodes.

Analyzing the Fig. 9, it can be noticed that for the nodal arrangement with many nodes, the relative error of the natural frequency is similar for different values of irregularity parameter (Cn=0.1 – 0.3) using the MLPG method.

5 Conclusions

The Meshfree Local Petrov-Galerkin (MLPG) method presented more accurate behavior that the Integrated Local Mesh free (ILMF) method for calculating the natural frequencies of the cantilever beam, mainly for the first value. The reference results were obtained using the FEM (ANSYS) with an extremely fine mesh.

The irregular nodal arrangement did not signifficatively influence the calculation of the natural frecuencies of the cantilever beam when 1261 nodes are used for the nodal discretization.

The methods used in this research for solving problems related with irregular nodal arrangement were efficient and accurate when local mesh free methods were used.

Acknowledgements. The program PECC – Posgraduacão em Estruturas e Construção Civil, Department of Civil and Environmental Engineering, Faculty of Technology, University of Brasilia.

Authorship statement. The authors hereby confirm that they are the sole liable persons responsible for the authorship of this work, and all material that has been herein included as part of the present paper is either the property of the authors and has the permission of the owners to be included here.

References

[1] Daxini, S. D. and Prajapati, J. M. A review on recent contribution of the meshfree methods to structure and fracture mechanics applications, the scientific word journal, 13 pages, 2014.
[2] Finalyson, B. A. The Method of Weighted Residuals and Vibrational Principles. Academic Press, 1972.
[3] Chen, J. S., Hillman, M. and Chi, S. W. Meshfree Methods: Progress made after 20 years, Journal of Engineering Mechanics 143, 4, 2017.
[4] Nayroles, B., Touzot, G. and Villon, P. Generalized the Finite Element Method: Diffuse Approximation and Diffuse Elements, Computational Mechanics 10, 307–318, 1992.
[5] Liu, W. K., Jun, S., and Zhang, Y.F. Reproducing Kernel Particle Methods, International Journal for Numerical methods in Engineering 20, 1081–1106, 2007.
[6] Belytshko, T., Lu, Y. Y. and Gu, L. Element – free Galerkin methods, International Journal for Numerical Methods in Engineering 37(2), 229–256, 1994.
[7] Atluri, S. N. and Zhu, T. A new Meshless Local Petrov-Galerkin (MLPG) approach in computational mechanics, Computational Mechanics 22(2), 117–127, 1998.
[8] Atluri, S. N. and Shen, S. The Meshless Local Petrov – Galerkin (MLPG) Method: A simple and Less-costly Alternative to the Finite Element and Boundary Element Methods, CMES: Computer Modeling in Engineering and Sciences 3(1), 11-51. 2002.
[9] Zhu, T., Zhang, J. and Atluri, S. N. A Local Boundary Integral Equation (LBIE) Method in Computational Mechanics and a Meshless Discretization Approach, Computational Mechanics 21, 223–235, 1998.
[10] Liu, G. R. and Gu, Y. T. A Local Point Interpolation Method for Stress Analysis of Two-Dimensional Solids, Structural Engineering and Mechanics 11(2), 221–236, 2001.
[11] Atluri, S. N. and Han, Z. D. and Rajendran, A. M. A New Implementation of the Meshless Finite Volume Method Through the MLPG Mixed Approach, CMES: Computer Modeling in Engineering and Sciences 6, 491-513, 2004.
[12] Oliveira, T. and Portela, A. Weak – Form Collocation – a Local Meshless Method in Linear Elasticity. Engineering Analysis with Boundary Elements 73, 144 – 160, 2016.
[13] Kirchhoff, G. Uber das Gleichgewicht und die Bewegung einer uendlich diinnen elastischen Stabes. J. Reine Angew. Math. v. 56, p.p. 285 – 313, 1859.
[14] Brebbia C. A. and Tottenham, H. Variational Basis of Aproximate Models in Continuum Mechanics. Southampton and Springer Verlag, 1985.
[15] Atluri, S. N. and Zhu, T. New Concepts in Meshless Methods, International Journal for Numerical Methods in Engineering 6, 537-556, 2000.
[16] LIU, G. R. e GU, Y. T. An introduction to meshfree methods and their programming. Springer Science & Business Media, 2005.